analytical chemistry

Article

pubs.acs.org/ac

Overcoming Sample Matrix Effect in Quantitative Blood Metabolomics Using Chemical Isotope Labeling Liquid Chromatography Mass Spectrometry

Deying Chen,[†] Wei Han,[‡] Xiaoling Su,[†] Liang Li,*[,†,‡] and Lanjuan Li*[,†]

[†]State Key Laboratory and Collaborative Innovation Center for Diagnosis and Treatment of Infectious Diseases, the First Affiliated Hospital, College of Medicine, Zhejiang University, Hangzhou, Zhejiang 310003, China

[‡]Department of Chemistry, University of Alberta, Edmonton, Alberta T6G 2G2, Canada

Supporting Information

ABSTRACT: Blood is widely used for discovery metabolomics to search for disease biomarkers. However, blood sample matrix can have a profound effect on metabolome analysis, which can impose an undesirable restriction on the type of blood collection tubes that can be used for blood metabolomics. We investigated the effect of blood sample matrix on metabolome analysis using a high-coverage and quantitative metabolome profiling technique based on differential chemical isotope labeling (CIL) LC-MS. We used ^{12}C-/^{13}C-dansylation LC-MS to perform relative quantification of the amine/phenol submetabolomes of four types of samples (i.e., serum, EDTA plasma, heparin plasma, and citrate plasma) collected from healthy individuals and compare their metabolomic results. From the analysis of 80 plasma and serum samples in experimental triplicate, we detected a total of 3651 metabolites with an average of 1818 metabolites per run (n = 240). The number of metabolites detected and the precision and accuracy of relative quantification were found to be independent of the sample type. Within each sample type, the metabolome data set could reveal biological variation (e.g., sex separation). Although the relative concentrations of some individual metabolites might be different in the four types of samples, for sex separation, all 66 significant metabolites with larger fold-changes (FC ≥ 2 and p < 0.05) found in at least one sample type could be found in the other types of samples with similar or somewhat reduced, but still significant, fold-changes. Our results indicate that CIL LC-MS could overcome the sample matrix effect, thereby greatly broadening the scope of blood metabolomics; any blood samples properly collected in routine clinical settings, including those in biobanks originally used for other purposes, can potentially be used for discovery metabolomics.

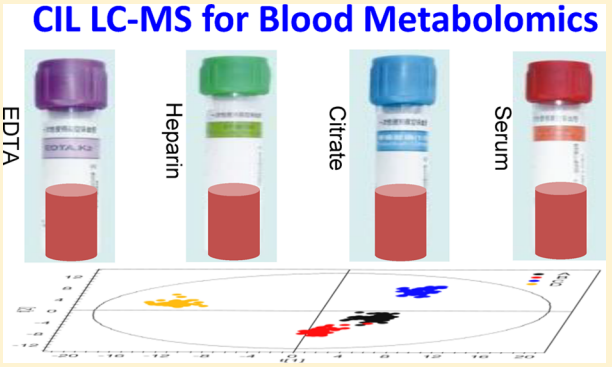

Blood samples are being extensively used in discovery metabolomics for finding sensitive and specific biomarkers of healthy and diseased states. To analyze the blood metabolome, LC-MS is widely used, because of its higher sensitivity than other techniques such as NMR and GC-MS.[1,2] However, different types of blood samples (i.e., serum and plasma prepared using different anticoagulants) have vastly different matrix compositions.[3] There is currently no consensus on which sample matrix works best for LC-MS-based metabolomics. Several studies have shown that experimental artifacts from the collection tubes (e.g., surfactants and anticoagulants) can be introduced to the measured metabolome profiles.[4−9] Metabolite detectability can also be significantly different from one sample matrix to another.[4−9] This matrix-dependence characteristic imposes an undesirable restriction on the type of samples useable for blood metabolomics. For example, many biobanks originally established for other purposes (e.g., for genomics research, longitudinal population-based health studies, and clinical trials of therapeutics)[10−13] with blood samples collected in tubes not ideal for current LC-MS-based metabolomics could not be used for discovery metabolomics. Thus, new techniques capable of performing quantitative and high-coverage analysis of metabolomic changes without the restriction of sample type are needed to extend blood metabolomics to a wide range of blood samples.

Recently, chemical isotope labeling (CIL) LC-MS has shown great promise for quantitative metabolomics with high metabolic coverage.[14−25] In particular, rationally designed isotope reagents with each targeting a chemical-group-based submetabolome, including amine,[14] carboxylic acid,[26] hydroxyl[27] and carbonyl groups,[28] have been developed. These four chemical groups cover more than 95% of the chemical structures in the Human Metabolome Database (HMDB), and thus, the combined results of the four groups can

Received: June 10, 2017
Accepted: August 8, 2017
Published: August 8, 2017

DOI: 10.1021/acs.analchem.7b02240
Anal. Chem. 2017, 89, 9424−9431

potentially reach over 95% of the entire metabolome. In this work, we present a study of using ^{12}C-/^{13}C-dansylation LC-MS to profile the amine/phenol submetabolome for investigating the blood sample matrix effect. The results shown herein indicate that CIL LC-MS can be used for analyzing any type of blood samples commonly collected in clinical laboratories with similar performance and is well-suited for quantitative and high-coverage blood metabolomics for biomarker discovery research.

EXPERIMENTAL SECTION

Figure 1 shows the study design and workflow for investigating the sample matrix effect on blood metabolomics. The study

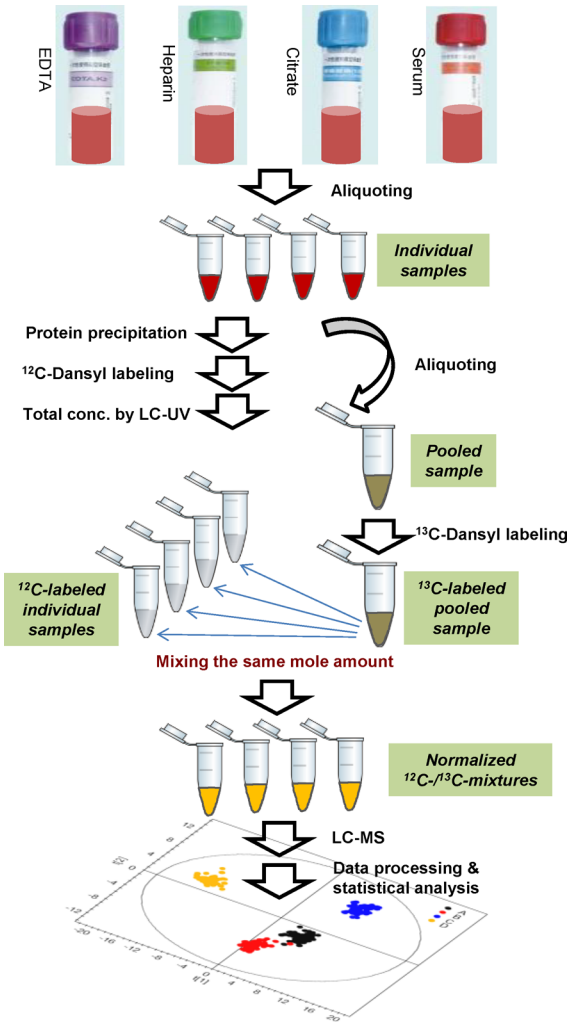

Figure 1. Workflow for investigating the blood matrix effect on metabolome analysis using differential CIL LC-MS. Blood was collected by venipuncture using a serum gel tube for processing into serum and potassium EDTA, lithium heparin, and sodium citrate tubes for processing into plasma. An aliquot of serum or plasma was taken for methanol precipitation of proteins, ^{12}C-dansylation labeling of the supernatant, and LC-UV measurement of the labeled metabolites. On the basis of LC-UV quantification results of individual ^{12}C-labeled samples, an equal mole amount of individual samples was taken and mixed to produce a pooled sample, which was then labeled using ^{13}C-dansylation. Equal mole amounts of ^{12}C-labeled sample and ^{13}C-labeled pool were mixed for LC-MS analysis. This workflow was also used for blood metabolomics where the same type of blood samples was used for measuring the metabolomic differences among the comparative individual samples.

protocol was approved by the Medical Ethics Committee of the first Affiliated Hospital of Zhejiang University, Hangzhou, China, and informed consents were obtained from all participants studied. Four types of tubes widely used in clinical laboratories for preparing plasma and serum samples were studied. They were BD Vacutainer K2 with 5.4 mg of EDTA, Vacutainer with 2.7 mL of 0.109 M Sodium Citrate, VACUETTE Tube LH with 6 mL of Lithium Heparin, and VACUETTE Z Serum Sep Clot Activator tubes coated with micronized silica particles which activate clotting. Since the amount of additives used in each tube is fixed, we did not investigate the effect of additive amounts on MS detection in this study. Overnight fasting blood (>12 h) was collected from 20 healthy individuals (10 males and 10 females) with similar characteristics of ethnicity (Chinese), age, weight, and BMI (Table S1). Blood was collected into four tubes with three types of anticoagulants (EDTA, heparin, and citrate) and one coagulant (Note S1-1). Each tube was processed and analyzed in experimental triplicate. In addition, blanks (i.e., tubes with the addition of an equivalent volume of water, instead of blood) were analyzed to determine the background signals from the matrices.

To profile the blood metabolomes from the four types of samples, each sample was labeled using ^{12}C-dansylation after protein precipitation (Note S1-2).[14] Briefly, 30 μL of plasma, serum, or blank was first mixed with 90 μL of cold methanol, vortexed, and then allowed to sit for 5 min. The sample was centrifuged at 18 000g for 15 min at room temperature. The supernatant was taken to a new 1.5 mL plastic vial and dried using Speedvac. The dried sample was then dissolved in 30 μL of H_2O and 15 μL of ACN, followed by adding 15 μL of buffer (sodium carbonate/sodium bicarbonate buffer at 500 mM with pH 9.4) and 30 μL of ^{12}C- or ^{13}C-dansyl chloride solution in ACN (20 mg/mL). The solution was mixed and incubated at 40 °C for 45 min. After that, 10 μL of NaOH solution (250 mM) was added and the mixture was incubated for another 10 min at 40 °C to quench the remaining dansyl chloride. In the end, 50 μL of formic acid (FA) in ACN/H_2O (425 mM) was added to neutralize the solution.

The resultant labeled sample was analyzed by LC-UV (Note S1-3) to measure the total concentration of labeled metabolites for sample amount normalization.[29] On the basis of the total concentration, an appropriate volume of an individual unlabeled sample was taken to mix with an equal mole amount of other unlabeled samples to generate a pooled sample which was then labeled by ^{13}C-dansylation. An equal mole amount of the ^{12}C-labeled individual sample and the ^{13}C-labeled pooled sample was mixed for LC-TOF-MS analysis (Note S1-4). A quality control (QC) sample was prepared by mixing an equal mole amount of the ^{12}C-labeled and ^{13}C-labeled pooled samples and injected into LC-MS after every 10 sample runs. We note that, in the dansylation labeling experiment of a sample, we cannot rule out the possibility of some metabolites being degraded (e.g., those degradable at pH 9.4). However, during the construction of a dansyl labeled standard library of 273 unique metabolites,[30] we labeled a metabolite standard one-by-one and did not observe chemical degradation or unexpected products of metabolites for these 273 standards.

The LC-MS data were processed using IsoMS,[31] Zero-fill,[32] and IsoMS-Quant[33] to generate the metabolite-peak-ratio table (Note S1-5). The final peak-ratio file containing metabolites consistently detected in more than 80% of the samples within the same tube group was exported to SIMCA-P+ 12.0 software

DOI: 10.1021/acs.analchem.7b02240
Anal. Chem. 2017, 89, 9424−9431

(Umetrics, Umeå, Sweden) for multivariate statistical analysis. Metabolite identification was performed based on mass and retention time match to the dansyl standard library using DnsID.[30] Putative identification was done on the basis of accurate mass matches to the metabolites in HMDB (8021 known human endogenous metabolites) and in the Evidence-based Metabolome Library (EML) (375 809 predicted human metabolites with one reaction) using MyCompoundID.[34] The mass accuracy tolerance window was set at 0.008 Da for database search.

RESULTS AND DISCUSSION

Serum and Plasma Submetabolomes. We used LC-UV to measure the total concentration of labeled metabolites for each processed sample. The average concentration was found to be almost the same for the four types of samples (Figure S1). Thus, from the perspective of a total amount of metabolites recovered, there was no bias toward any one particular sample type for blood processing.

We then compared the LC-MS results of the ^{12}C-/^{13}C-labeled plasma and serum samples. Figure 2 shows the ion chromatograms of EDTA plasma, heparin plasma, citrate plasma, and serum of the same subject with each ^{12}C-labeled sample mixed with the ^{13}C-labeled pool. The chromatograms appear to be very similar, suggesting that the metabolome profiles of the four samples were similar. This is different from the reported results obtained using conventional LC-MS.[4−9] These studies showed that the chromatograms obtained from plasma and serum were significantly different and there were strong matrix effects on metabolite detection (i.e., detecting different metabolites with different intensities in plasma and serum). In our work, metabolites were labeled with a common and relatively large dansyl group, and thus, the chemical and physical properties of the labeled metabolites are strongly influenced by the dansyl group. As a result, the properties of dansylated metabolites are much more similar, compared to the unlabeled metabolites. Consequently, the ionization efficiencies and ion suppression effects of the labeled metabolites become similar. Thus, the detectability of the labeled metabolites has much less dependence on the sample matrix, resulting in similar LC-MS detection behavior of the four types of samples as shown in Figure 2.

It should be noted that, in CIL LC-MS quantitative metabolomics workflow, we perform relative quantification to determine the metabolite concentration differences (i.e., fold-changes) between two or more groups of samples using ^{13}C-labeled pool as the internal control. Thus, individual isotope standards, which are often required for absolute quantification of targeted analytes, are not needed. However, if absolute quantification of an individual metabolite is required, previous studies have shown that concentrations of amino acids, polyphenols, and other analytes using isotope labeled standards could be determined with high accuracy and precision.[14,35,36] CIL LC-MS is also different from external calibration, which is useful for analyzing a small number of targeted metabolites with the available standards; CIL LC-MS can be used to measure the relative concentration changes of all the metabolites in a submetabolome.

We have examined the matrix effect on the detectability of individual metabolites. One example is shown in Figure S2A where the molecular ion regions of the same peak pair obtained from the four tubes are shown. The absolute signal intensities and their peak ratios were similar in the four types of samples.

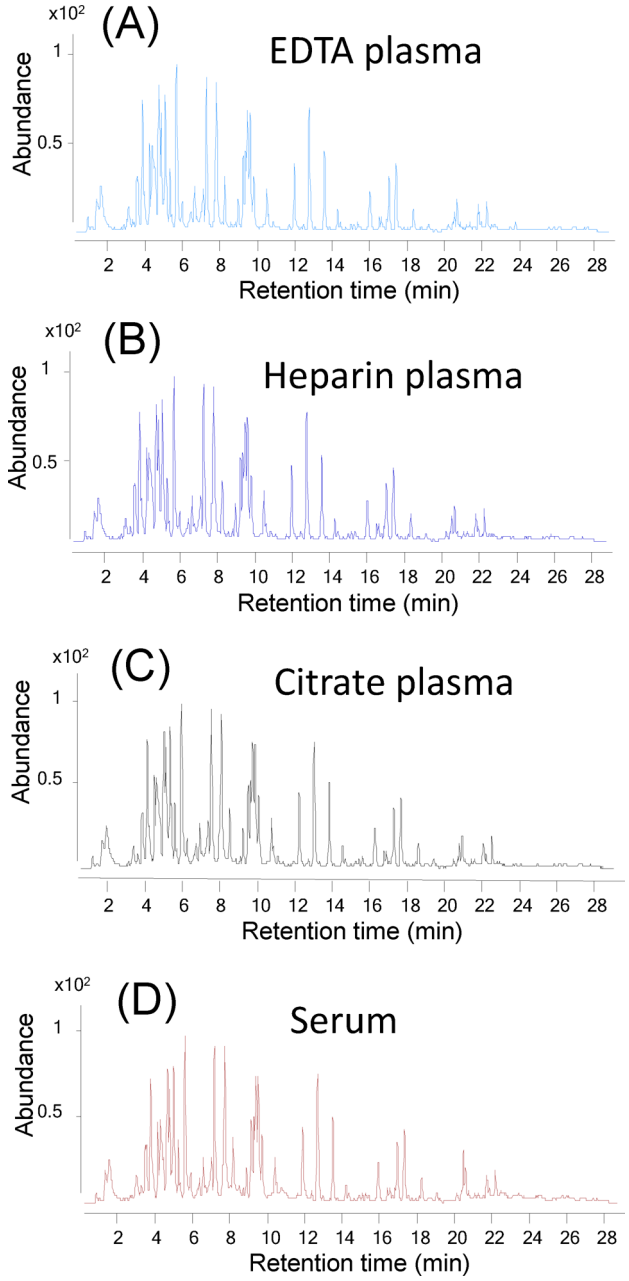

Figure 2. LC-MS ion chromatograms of ^{12}C-labeled sample mixed with ^{13}C-labeled pool prepared from (A) EDTA plasma, (B) heparin plasma, (C) citrate plasma, and (D) serum of the same individual. The ^{13}C-labeled pool, representing the average plasma/serum metabolome of all the samples (blood of 20 subjects with each collected in four tubes), was used as a global control or standard for relative quantification of ^{12}C-labeled samples.

In contrast, Figure S2B shows an example where the absolute signal intensities were altered in two of the four types of samples. In this case, the EDTA plasma and the citrate plasma gave similar intensities, but the serum and the heparin plasma gave lower intensities. Globally, we plot the distributions of the absolute intensities of all the peak pairs detected in the four types of samples collected from a subject (Figure 3A). This plot provides an overview of the detectability of the submetabolomes in four tubes. It is clear that the distributions are very similar, indicating that for most of the labeled metabolites, their

DOI: 10.1021/acs.analchem.7b02240
Anal. Chem. 2017, 89, 9424−9431

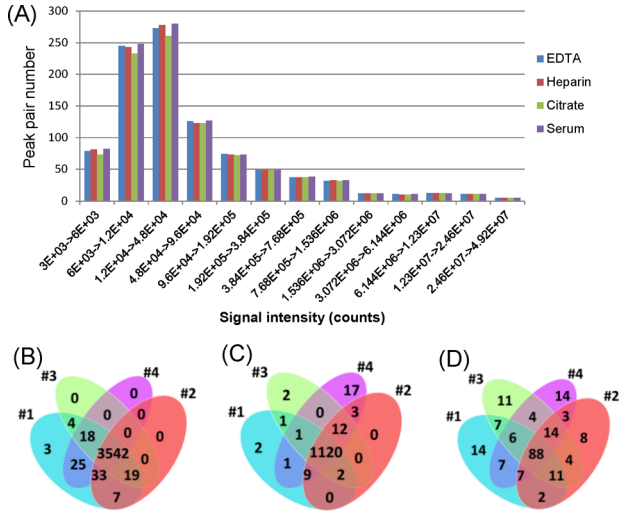

Figure 3. (A) Number of peak pairs at different ranges of absolute MS signal intensity detected in four types of samples from the same individual. Venn diagrams of the numbers of peak pairs showing (B) all the samples, (C) 80% of the samples within each type, and (D) four blank tubes: #1: EDTA plasma; #2: heparin plasma; #3: citrate plasma; #4: serum.

absolute intensities do not change much across different sample types.

The above finding is further supported by examining the commonality in the metabolites detected from the four tubes. Figure 3B shows the distribution of the numbers of labeled metabolites detected in the four tubes. From the combined results of the 240 samples analyzed, a total of 3651 metabolites were detected. Among them, 3651 (100%) were detected in EDTA plasma (1811 ± 196 per run, n = 60), 3601 (98.6%) in heparin plasma (1845 ± 166 per run, n = 60), 3583 (98.1%) in citrate plasma (1780 ± 188 per run, n = 60), and 3618 (99.1%) in serum (1836 ± 163 per run, n = 60). If only the metabolites commonly detected in >80% of the samples of a given type were considered (this 80% rule was applied to retain the metabolites for statistical analysis in this study), there were still 1136, 1146, 1138, and 1163 metabolites detected from EDTA plasma, heparin plasma, citrate plasma, and serum, respectively, with a combined list of 1170 metabolites. Figure 3C shows the number distribution of these more reproducibly detected metabolites. Among the 1170 metabolites, 97.1%, 97.9%, 97.3%, and 99.4% of them were detectable in EDTA plasma, heparin plasma, citrate plasma, and serum, respectively. By comparison, there were only 142, 137, 145, and 143 peak pairs in the corresponding blanks (Figure 3D) with 88 pairs commonly detected in all the blanks (Note S2-1 describes the identification of a few of these background chemicals). Thus, the background contribution from the tubes to the blood metabolome was not significant. The results shown in Figure 3B–C indicate that the number of metabolites detected was almost the same from the four types of blood samples and a vast majority of them could be commonly detected in these samples.

For a combined list of 3651 peak pairs detected in all the samples, we identified 78 metabolites using the dansyl library (Table S2A), matched 883 peak pairs using accurate mass search to the HMDB library (Table S2B) and matched 1746 peak pairs to the EML library of predicted metabolites (Table S2C). Thus, 2707 out of the 3651 peak pairs (74.1%) could be either positively identified or mass-matched to some metabolite structures. The 944 unmatched peak pairs are listed in Table S2D.

Taken together, the above results from LC-UV and LC-MS analyses indicate that the detection of the amine/phenol submetabolome was not significantly affected by the sample type. This is in direct contrast to the conventional nonlabeling LC-MS approach where metabolite detectability has been shown to be strongly dependent on the blood sample matrix. Moreover, the number of metabolites detected in CIL LC-MS is much higher than conventional LC-MS, due to much increased ionization efficiency after chemical labeling. The use of other labeling chemistries targeting the acid, hydroxyl, and carbonyl submetabolomes should further increase the coverage.

Relative Quantification of the Submetabolomes. Besides the need of high-coverage metabolite detection, blood metabolomics requires accurate relative quantification of individual metabolites in comparative samples. In CIL LC-MS, a ^{13}C-labeled pool is used as a control or global standard and a same mole amount of the labeled pool is spiked into all individual ^{12}C-labeled samples for relative quantification. While matrix effect can influence the absolute intensity of a detected peak in MS, the relative peak intensity within a peak pair of a given metabolite does not change much (see Figure S2 as an example). This is because the ^{12}C-labeled peak from an individual sample experienced the same matrix effect as that of the ^{13}C-labeled peak from the pooled sample. Concerning potential matrix effect on the labeling efficiency of a metabolite, the individual samples and the pooled sample have similar metabolite composition (concentrations of individual metabolites and chemical diversity) and matrix (e.g., for serum sample analysis, the individual samples are serum and the pooled sample prepared from mixing individual samples is also serum). Thus, during the labeling process, an analyte to be labeled is subjected to a very similar matrix effect, which does not cause significant variation in labeling efficiency, as we have illustrated previously.[37]

At the global submetabolome level, we have examined the overall experimental reproducibility of our data set. In our work, we performed triplicate experiments for each sample, and thus, the relative standard deviation (RSD) of an individual peak pair commonly detected in all triplicates could be calculated. In Figure 4, we present the triplicate data of the four types of samples collected from the same subject where the experimental variation of each peak pair is shown by the RSD value. To study the matrix effect on both the absolute quantification and the relative quantification, we calculated the RSD of the absolute intensities of the ^{12}C-labeled peaks and the RSD of the peak pair ratios of an individual metabolite detected in triplicates. Figure 4A shows a plot of the number of peak pairs as a function of the RSD values of peak pairs commonly detected in all four tubes. It is clear that much higher precision is obtained by using peak ratio measurement, compared to absolute intensity measurement. Figure 4B–E shows the same type of plot for each sample type. In all cases, precision is improved by using the relative quantification method. These plots also show that the absolute intensity distribution is almost the same for the four tubes, suggesting again that there were no overall bias in detectability. Since the precision differences are small among the four sample types, all the tubes can be used for metabolomic analysis if peak ratio measurement is used.

DOI: 10.1021/acs.analchem.7b02240
Anal. Chem. 2017, 89, 9424–9431

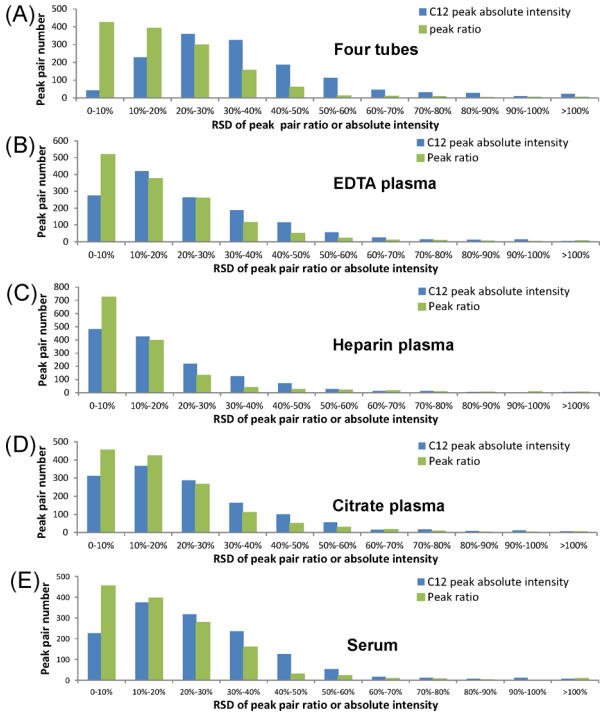

Figure 4. Number of peak pairs as a function of RSD values of peak ratios or absolute intensity (n = 3) of individual pairs commonly detected in (A) all four types of samples of one individual, (B) EDTA plasma, (C) heparin plasma, (D) citrate plasma, and (E) serum.

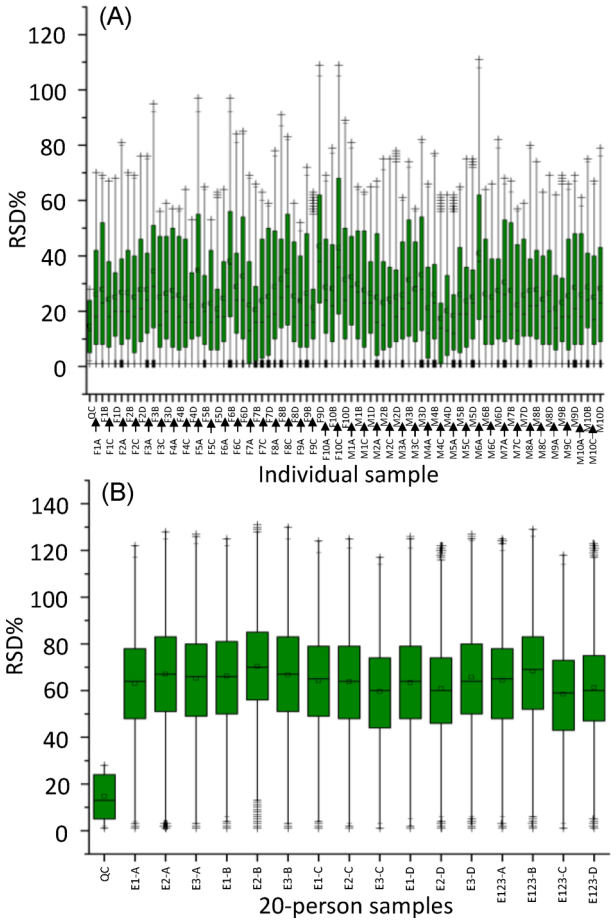

Figure 5. (A) Box plots of RSD values of peak ratios of individual pairs commonly detected in experimental triplicates of each sample coded as xyz where x = F for female or M for male; y = 1 to 10 for subject #1 to subject #10; z = A for EDTA plasma, B for heparin plasma, C for citrate plasma, and D for serum (e.g., F1A refers to the sample from female, subject #1, EDTA plasma). QC is the quality control sample. (B) Box plots of RSD values of peak ratios of individual pairs commonly detected in one or all replicate analysis of 20 subjects with blood samples collected in one type of tube (the y-axis label, Ex-y, where x = 1, 2, 3, or 123 and y = A–D, refers to the RSD data from replicates #1, #2, #3, or all triplicates in tubes A, B, C, or D). The RSD box plot of QC measures injection variations in LC-MS (n = 24), the box plot of individual sample measures the experimental variations (n = 3), and the box plot of 20-person-samples measures the biological and experimental variations (n = 20 for one replicate and n = 60 for triplicates).

To investigate the experimental variation of peak ratios determined from triplicate analysis of an individual sample (80 samples from 20 subjects with each blood collected in four tubes), we calculated the RSD values of the peak pairs detected in each sample (n = 3) and used the box plot to plot the distribution of these RSD values. Figure 5A shows the box plots of RSD values for the QC samples (n = 24) and 80 blood samples (note that, in the y-axis, sample number is coded as, e.g., F1A denoting female, subject #1, blood sample collected in tube A or EDTA plasma). The QC data have low RSDs with a median of 7% and an interquartile range (IQR) from 4% (first quartile) to 12% (third quartile). In comparison, the average of the medians for the 80 samples is 15% with the average first quartile value of 8% and the average third quartile value of 24%. Thus, the RSDs of triplicate analysis of the real samples are almost doubled, compared to the QC result. This is expected as the experimental triplicates in a sample account for the accumulated variation from the entire experimental workflow, while injection replicate runs in QC only account for the instrumental variation in data collection. Figure 5A shows that the RSD median and IQR values from all the 80 samples are similar, indicating that similar experimental variations were found in analyzing these samples.

For the samples collected from different subjects, the relative quantification results of the peak pairs detected should reflect biological variations as well as experimental variations. To reveal the true biological variations, experimental variations from an analytical method must be smaller than the biological variations. As indicated earlier, in our work, four different tubes were used to collect and process blood samples of 20 individuals with each sample analyzed in experimental triplicate. We calculated the RSD of the same peak pair found in each experimental replicate of 20 blood samples collected in one of the four tubes. Figure 5B shows the box plots of the RSDs from 12 data sets of triplicate analysis of four types of 20-subject samples (in y-axis, each data set is coded as, e.g., E1-A denoting experimental replicate #1, 20 blood samples collected in tube A or EDTA plasma). For these 12 data sets, the average of the median RSD values is 43% with the average first quartile value of 29% and the average third quartile value of 57%. If the experimental triplicate data from each tube are combined, four data sets from the four tubes are generated and each box plot of the RSDs is shown in Figure 5B (in y-axis, (E123)-A, for example, denotes the combined triplicate analysis from tube A or EDTA plasma). For these 4 data sets, the average of the median RSD values is 36% with the average first quartile value of 16% and the average third quartile value of 50%. Figure 5B clearly shows that the RSD values of peak ratios of individual

DOI: 10.1021/acs.analchem.7b02240
Anal. Chem. 2017, 89, 9424–9431

metabolites for 20 subjects are much greater than those of experimental triplicates, indicating that the biological variations are much greater than the experimental variations. Thus, the dansylation LC-MS method is sufficiently accurate and precise to afford the detection of biological variations among the 20 subjects. In the following section, we explore the use of the metabolomic data to reveal the biological variations, i.e., sex separation, in a small, but relatively homogeneous, sample set with a main objective of determining whether the common significant metabolites are found in four types of samples.

Statistical Analysis of Different Tubes and Sex Separation. Figure 6A shows the PCA plot of the amine/phenol submetabolome data set obtained from the blood samples collected in four tubes as well as the QC samples. The QC data cluster together tightly. The four types of samples are separated from each other, which can be more clearly seen in the OPLS-DA plot shown in Figure 6B. These results indicate that there are some differences in the measured metabolomes of the four samples. In our samples of 10 males and 10 females with similar ages, BMIs, and ethnicities, an obvious group separation is based on sex. Figure 6C shows the PCA plot of the same data set as that used in Figure 6A but color-coded differently into female-plasma, male-plasma, female-serum, and male-serum. Figure 6D shows the corresponding OPLS-DA plot. The sex separation can already be seen in the PCA plot and becomes very clear in the OPLS-DA plot. However, as Figure 6C shows, tube type can influence the separation. Therefore, it is important to use the same type of blood collection tube for revealing biological variations. For comparison, we generated the PCA and OPLS-DA plots of the same data set using absolute intensities of ^{12}C-labeled metabolites (see Figure 7), instead of using the peak ratios of ^{12}C-labeled metabolites vs ^{13}C-labeled pool (Figure 6). Figures 6 and 7 show that, using the ratio values, within a group the data points are clustered more tightly together and between groups the point separation is much clearer. The higher performance can be attributed to much improved precision and accuracy for relative quantification using peak ratios (see, for example, Figure 4), compared to using absolute intensities. The question is, even with the use of ratio values for relative quantification, whether the use of different tubes will lead to the discovery of the same set of significant metabolites.

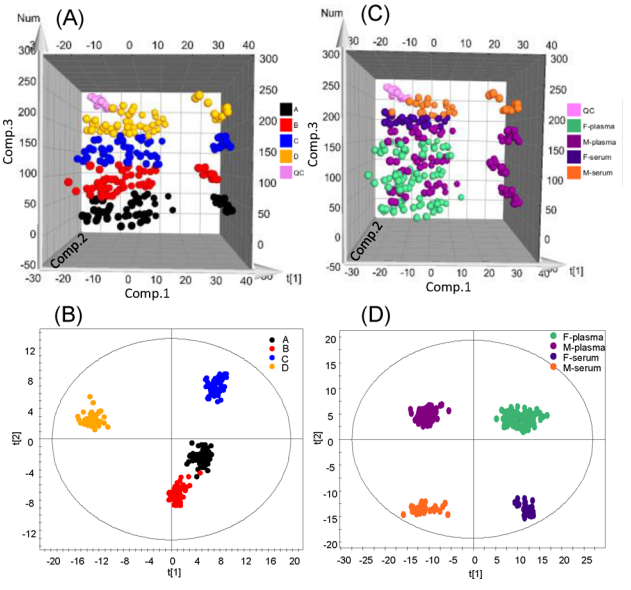

Figure 6. (A) PCA plot of the QC samples and the 80 samples from 20 subjects with blood collected in four types of tubes and (B) OPLS-DA plot of the 80 samples color-coded with A for EDTA plasma, B for heparin plasma, C for citrate plasma, and D for serum. (C) PCA plot of the QC and 80 samples and (D) OPLS-DA plot of the 80 samples color-coded according to sex and serum or plasma with F = female and M = male. The binary metabolomic comparison of females vs males for each same type is shown in Figure S3 (PCA and OPLS-DA plots) and Figure S4 (volcano plots).

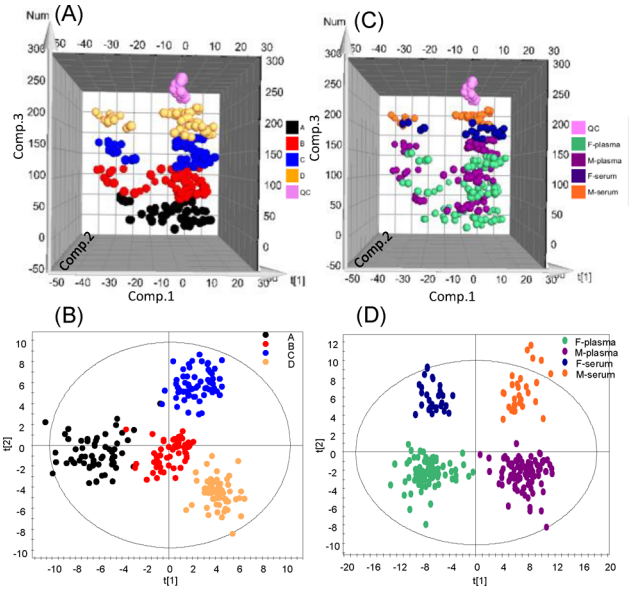

Figure 7. (A, C) PCA plots and (B, D) OPLS-DA plots of the same data set as those in Figure 6, but using the absolute intensity values of ^{12}C-labeled metabolites, instead of the peak ratio values of ^{12}C-labeled metabolites vs ^{13}C-labeled pool.

To address this question, we performed a binary comparison of the metabolomes of males and females using the same type of samples with the resultant PCA and OPLS-DA plots shown in Figure S3. Even in the PCA plots, a clear separation between males and females is observed. To determine the metabolites that contribute to separation of the two groups, we defined a significant metabolite as the one found to be significant in both multivariate analysis using OPLS-DA and univariate analysis using the volcano plot. On the basis of OPLS-DA analyses, the number of significant metabolites with a VIP score of ≥1.5 was found to be 133, 134, 130, and 127 from EDTA plasma, heparin plasma, citrate plasma, and serum, respectively (see Table S3 for the lists). In the volcano plots of sex separation in four types of samples, two levels of fold-change (FC) threshold (≥1.5 or 2) were plotted (Figure S4). The numbers of significant metabolites were 170, 222, 196, and 217 using FC ≥ 1.5 with $p < 0.05$ and 46, 72, 60, and 69 using FC ≥ 2 with $p < 0.05$ (see Table S4 for the lists). To avoid overfitting in multiple testing, the false discovery rate (q-value) calculated by the Storey and Tibshirani method was found to be 3.54%, 3.10%, 3.14%, and 3.28%, respectively, with $p < 0.05$. From the volcano plot (FC ≥ 1.5) and its corresponding OPLS-DA analysis (VIP score ≥1.5), we determined the number of common significant metabolites to be 91, 101, 89, and 92 for EDTA plasma, heparin plasma, citrate plasma, and serum, respectively (Table S5).

DOI: 10.1021/acs.analchem.7b02240
Anal. Chem. 2017, 89, 9424−9431

Figure S5 shows the Venn diagrams for comparing the numbers of significant metabolites found from four types of samples. At FC ≥ 1.5, there are 26 significant metabolites commonly found from the samples collected in four different tubes. If we only compare the three plasma samples, there are 37 common significant metabolites found with FC ≥ 1.5. At FC ≥ 2, there are 20 significant metabolites commonly found in four tubes. If we only compare the three plasma samples, there are 21 common significant metabolites found with FC ≥ 2.

For clinical application of a true biomarker, the greater the fold-change between two groups of samples, the better and easier using the biomarker to separate the two groups. Thus, if we only focus on the metabolites with FC ≥ 2, according to Figure S5B, we have a total of 66 metabolites with FC ≥ 2 found in the data set produced from at least one tube. All 66 significant metabolites can be found in any tube with similar or reduced, but still statistically significant, fold-changes (see Note S2-2 for fold-change comparison). These results suggest that, for discovery metabolomics to find the clinically useful biomarkers with relatively large fold changes from one group to another, all the sample types could potentially be used. The box plots of some significant metabolites for sex separation and their identities are shown in Notes S2-3 and S2-4.

CONCLUSIONS

We have shown that using differential CIL LC-MS, blood samples commonly collected and processed in clinical settings (i.e., serum, EDTA plasma, heparin plasma, and citrate plasma), including those in biobanks originally collected for other research purposes, are suitable for blood metabolomics. Among the four types of samples, there is no significant difference in metabolite detectability and relative quantification precision. Although the use of the same type of samples is preferred to reveal biological variations among comparative groups, similar significant metabolites for separating biological variations (e.g., sex separation) can be found in metabolomic comparisons of four types of samples. It is shown that, in all samples, ^{12}C-/^{13}C-dansylation LC-MS targeting the amine/phenol submetabolome allows the profiling of thousands of metabolites. This coverage is expected to increase when other labeling chemistries targeting the acid, hydroxyl, and carbonyl submetabolomes are applied to the blood sample.

It should be noted that the experimental design and workflow used in this study should be applicable to investigate and compare other types of blood collection tubes specially designed for metabolomics research. For example, various protease inhibitors can be added to blood collection tubes to prevent metabolism during blood collection and storage.[3,38] In future work, we will compare the performance of conventional blood collection tubes and specially designed tubes for quantitative metabolomics, which would benefit our understanding of how some metabolites might change during sample collection and storage. If a biomarker found for a particular disease is among these readily changeable metabolites, we might avoid the use of this biomarker in a routine clinical laboratory, unless a special type of collection tube is used for blood collection.

ASSOCIATED CONTENT

Supporting Information

The Supporting Information is available free of charge on the ACS Publications website at DOI: 10.1021/acs.analchem.7b02240.

Supplemental Note S1 for experimental section, Note S2 for results, Figures S1−S5 for comparison results, and Tables S1−S7 listing metabolites and metabolite identification results (PDF)

AUTHOR INFORMATION

Corresponding Authors

*E-mail: Liang.Li@ualberta.ca.
*E-mail: ljli@zju.edu.cn.

ORCID

Liang Li: 0000-0002-9347-2108

Notes

The authors declare no competing financial interest.

ACKNOWLEDGMENTS

This collaborative research was in part supported by a visiting professorship to Liang Li by Zhejiang University K. P. Chao's Hi-Tech Foundation for Scholars and Scientists. Additional support was provided by the Natural Sciences and Engineering Research Council of Canada, Canadian Institutes of Health Research, Canada Research Chairs, Genome Canada and Alberta Innovates, Independent Project Fund of the State Key Laboratory for Diagnosis and Treatment of Infectious Disease (SKL DTID), Foundation of SKL and Collaborative Innovation Center for DTID, and The First Affiliated Hospital of Medical College of Zhejiang University (Grant No. 2014KF04).

REFERENCES

(1) Ortmayr, K.; Causon, T. J.; Hann, S.; Koellensperger, G. *TrAC, Trends Anal. Chem.* **2016**, *82*, 358−366.
(2) Kohler, I.; Giera, M. *J. Sep. Sci.* **2017**, *40*, 93−108.
(3) Yin, P. Y.; Lehmann, R.; Xu, G. W. *Anal. Bioanal. Chem.* **2015**, *407*, 4879−4892.
(4) Wedge, D. C.; Allwood, J. W.; Dunn, W.; Vaughan, A. A.; Simpson, K.; Brown, M.; Priest, L.; Blackhall, F. H.; Whetton, A. D.; Dive, C.; Goodacre, R. *Anal. Chem.* **2011**, *83*, 6689−6697.
(5) Yin, P. Y.; Peter, A.; Franken, H.; Zhao, X. J.; Neukamm, S. S.; Rosenbaum, L.; Lucio, M.; Zell, A.; Haring, H. U.; Xu, G. W.; Lehmann, R. *Clin. Chem.* **2013**, *59*, 833−845.
(6) Yu, Z. H.; Kastenmuller, G.; He, Y.; Belcredi, P.; Möller, G.; Prehn, C.; Mendes, J.; Wahl, S.; Roemisch-Margl, W.; Ceglarek, U.; Polonikov, A.; Dahmen, N.; Prokisch, H.; Xie, L.; Li, Y. X.; Wichmann, H. E.; Peters, A.; Kronenberg, F.; Suhre, K.; Adamski, J.; Illig, T.; Wang-Sattler, R. *PLoS One* **2011**, *6*, e21230.
(7) Zhou, Z.; Chen, Y. H.; He, J. M.; Xu, J.; Zhang, R. P.; Mao, Y.; Abliz, Z. *Bioanalysis* **2017**, *9*, 239−250.
(8) Barri, T.; Dragsted, L. O. *Anal. Chim. Acta* **2013**, *768*, 118−128.
(9) Denery, J. R.; Nunes, A. A. K.; Dickerson, T. J. *Anal. Chem.* **2011**, *83*, 1040−1047.
(10) Ellervik, C.; Vaught, J. *Clin. Chem.* **2015**, *61*, 914−934.
(11) Halim, S. A.; Newby, L. K.; Ohman, E. M. *Clin. Chem.* **2012**, *58*, 45−53.
(12) Hebels, D.; Georgiadis, P.; Keun, H. C.; Athersuch, T. J.; Vineis, P.; Vermeulen, R.; Portengen, L.; Bergdahl, I. A.; Hallmans, G.; Palli, D.; Bendinelli, B.; Krogh, V.; Tumino, R.; Sacerdote, C.; Panico, S.; Kleinjans, J. C. S.; de Kok, T.; Smith, M. T.; Kyrtopoulos, S. A.; EnviroGenomarkers Project Consortium. *Environ. Health Perspect.* **2013**, *121*, 480−487.
(13) Rankin, N. J.; Preiss, D.; Welsh, P.; Sattar, N. *Int. J. Epidemiol.* **2016**, *45*, 1351−1371.
(14) Guo, K.; Li, L. *Anal. Chem.* **2009**, *81*, 3919−3932.
(15) Dai, W. D.; Huang, Q.; Yin, P. Y.; Li, J.; Zhou, J.; Kong, H. W.; Zhao, C. X.; Lu, X.; Xu, G. W. *Anal. Chem.* **2012**, *84*, 10245−10251.

DOI: 10.1021/acs.analchem.7b02240
Anal. Chem. 2017, 89, 9424−9431

(16) Leng, J. P.; Wang, H. Y.; Zhang, L.; Zhang, J.; Wang, H.; Guo, Y. L. *Anal. Chim. Acta* **2013**, *758*, 114−121.
(17) Tayyari, F.; Gowda, G. A. N.; Gu, H. W.; Raftery, D. *Anal. Chem.* **2013**, *85*, 8715−8721.
(18) Yuan, W.; Edwards, J. L.; Li, S. W. *Chem. Commun.* **2013**, *49*, 11080−11082.
(19) Mochizuki, T.; Todoroki, K.; Inoue, K.; Min, J. Z.; Toyo'oka, T. *Anal. Chim. Acta* **2014**, *811*, 51−59.
(20) Chu, J. M.; Qi, C. B.; Huang, Y. Q.; Jiang, H. P.; Hao, Y. H.; Yuan, B. F.; Feng, Y. Q. *Anal. Chem.* **2015**, *87*, 7364−7372.
(21) Arrivault, S.; Guenther, M.; Fry, S. C.; Fuenfgeld, M.; Veyel, D.; Mettler-Altmann, T.; Stitt, M.; Lunn, J. E. *Anal. Chem.* **2015**, *87*, 6896−6904.
(22) Wong, J. M. T.; Malec, P. A.; Mabrouk, O. S.; Ro, J.; Dus, M.; Kennedy, R. T. *J. Chromatogr A* **2016**, *1446*, 78−90.
(23) Yu, L.; Ding, J.; Wang, Y. L.; Liu, P.; Feng, Y. Q. *Anal. Chem.* **2016**, *88*, 1286−1293.
(24) Hao, L.; Johnson, J.; Lietz, C. B.; Buchberger, A.; Frost, D.; Kao, W. J.; Li, L. J. *Anal. Chem.* **2017**, *89*, 1138−1146.
(25) Fan, R. J.; Guan, Q.; Zhang, F.; Leng, J. P.; Sun, T. Q.; Guo, Y. L. *Anal. Chim. Acta* **2016**, *908*, 132−140.
(26) Guo, K.; Li, L. *Anal. Chem.* **2010**, *82*, 8789−8793.
(27) Zhao, S.; Luo, X.; Li, L. *Anal. Chem.* **2016**, *88*, 10617−10623.
(28) Zhao, S.; Dawe, M.; Guo, K.; Li, L. *Anal. Chem.* **2017**, *89*, 6758−6765.
(29) Wu, Y. M.; Li, L. *Anal. Chem.* **2012**, *84*, 10723−10731.
(30) Huan, T.; Wu, Y. M.; Tang, C. Q.; Lin, G. H.; Li, L. *Anal. Chem.* **2015**, *87*, 9838−9845.
(31) Zhou, R.; Tseng, C. L.; Huan, T.; Li, L. *Anal. Chem.* **2014**, *86*, 4675−4679.
(32) Huan, T.; Li, L. *Anal. Chem.* **2015**, *87*, 1306−1313.
(33) Huan, T.; Li, L. *Anal. Chem.* **2015**, *87*, 7011−7016.
(34) Li, L.; Li, R. H.; Zhou, J. J.; Zuniga, A.; Stanislaus, A. E.; Wu, Y. M.; Huan, T.; Zheng, J. M.; Shi, Y.; Wishart, D. S.; Lin, G. H. *Anal. Chem.* **2013**, *85*, 3401−3408.
(35) Peng, J., St; Laurent, C. D.; Befus, A. D.; Zhou, R. K.; Li, L. *Metabolomics* **2014**, *10*, 1305−1317.
(36) Achaintre, D.; Bulete, A.; Cren-Olive, C.; Li, L.; Rinaldi, S.; Scalbert, A. *Anal. Chem.* **2016**, *88*, 2637−2644.
(37) Han, W.; Li, L. *Metabolomics* **2015**, *11*, 1733−1742.
(38) Bielohuby, M.; Popp, S.; Bidlingmaier, M. *Mol. Metab.* **2012**, *1*, 47−60.

DOI: 10.1021/acs.analchem.7b02240
Anal. Chem. 2017, 89, 9424−9431